Acta Crystallographica Section A
Foundations of Crystallography
ISSN 0108-7673

Received 5 March 2004
Accepted 26 July 2004

Modeling of the nuclear parameters for H atoms in X-ray charge-density studies

Anders Østergaard Madsen,[a,b] Henning Osholm Sørensen,[a] Claus Flensburg,[c] Robert F. Stewart[d] and Sine Larsen[a,b]*

[a]Centre for Crystallographic Studies, Department of Chemistry, University of Copenhagen, Universitetsparken 5, DK-2100 Copenhagen, Denmark, [b]ESRF, BP 220, F-38043 Grenoble CEDEX, France, [c]Global Phasing Ltd, Sheraton House, Castle Park, Cambridge CB3 0AX, England, and [d]Department of Chemistry, Carnegie Mellon University, 4400 Fifth Avenue, Pittsburgh, PA 15321, USA. Correspondence e-mail: slarsen@esrf.fr

Extensive and precise X-ray diffraction data for xylitol have been used to test different approaches to estimate nuclear parameters for H atoms in charge-density studies. The parameters from a neutron diffraction study of the same compound were taken as a reference. The resulting static charge densities obtained for the different approaches based on a multipole model were subjected to a topological analysis. The comparative analysis led to the following results. The procedure of extending the X—H bond to match bond lengths from neutron diffraction studies provides the best agreement with the neutron positional parameters. An isotropic model for the atomic displacements of H atoms is highly unsatisfactory and leads to significant deviations for the properties of the bond critical points including those that only involve non-H atoms. Anisotropic displacement parameters for H atoms can be derived from the X-ray data that are in agreement with the values from the neutron study, and the resulting charge-density models are in good agreement with the reference model. The anisotropic displacement parameters for H atoms are derived from the X-ray data as a sum of the external (rigid-body) and internal vibrations. The external vibrations are obtained from a **TLS** analysis of the ADPs of the non-H atoms and the internal vibrations from analysis of neutron diffraction studies of related compounds. The results from the analysis of positional and thermal parameters were combined to devise a 'best anisotropic' model, which was employed for three other systems where X-ray and neutron data were available. The results from the topological analysis of these systems confirm the success of the 'best anisotropic' model in providing parameters for the H atoms that give charge densities in agreement with the reference models based on H-atom parameters derived from neutron diffraction.

1. Introduction

The majority of recent studies on crystal charge densities based on accurate X-ray diffraction data have focused on properties derived from the static crystal electron density. It is the experimental thermally averaged charge density that is obtained from the diffraction experiment, and the deconvolution of the thermal motion to obtain the static electron density requires reliable parameters for all types of atoms including the H atoms. Supplementing the X-ray diffraction investigation with a neutron diffraction study in order to obtain the H-atom positional and thermal parameters is not always possible due to difficulties in obtaining sufficiently large crystals and the limited access to neutron sources. Therefore, most studies have to employ models for the H atoms exclusively based on X-ray diffraction data.

Refinement against X-ray data leads to an apparent shortening of the bond lengths involving H atoms. This can be compensated for by changing the positional parameters so that they maintain the direction of the bond, which is elongated to match equivalent bond lengths from neutron diffraction studies. It is much more complicated to obtain a model for the atomic displacement parameters for the H atoms. Many recent charge-density studies have employed the simplest model, namely isotropic displacement parameters. The approach to obtain anisotropic displacement parameters for H atoms was pioneered by Hirshfeld and co-workers (Harel & Hirshfeld, 1975; Hirshfeld, 1976; Hirshfeld & Hope, 1980; Eisenstein & Hirshfeld, 1983). The anisotropic displacement parameters for the H atoms were estimated as a combination of contributions from rigid-body motion and internal vibrations assuming that the two types of motion are

uncorrelated. Parameters describing the rigid-body motion can be obtained from a (segmented) rigid-body model based on the non-H-atom ADPs, while the internal vibrations can be derived from *ab initio* calculations (Flaig *et al.*, 1998), assigned on the basis of 'spectroscopic evidence' (Hirshfeld & Hope, 1980; Destro & Merati, 1995; Roversi *et al.*, 1996), or on the basis of rigid-body analyses of similar compounds studied by neutron diffraction (Chen & Craven, 1995). The most recent work along these lines is by Roversi & Destro (2004). They obtained approximate anisotropic displacement parameters for H atoms as a sum of the external and internal mean square motions. The former was derived from rigid-body analysis of the ADPs for the non-H atoms, and the latter from solid-state infrared spectra. The estimated ADPs for 1-methyluracil were found to be in good agreement with the parameters obtained by neutron diffraction.

Recently, it has been shown (Bürgi & Capelli, 2000; Capelli *et al.*, 2000) how multi-temperature studies can be used to assign the atomic mean square displacements to rigid-body and internal vibrations. By using neutron diffraction results for C_6D_6 at several temperatures, this method was elegantly used to assign mean square displacements to the H atoms in benzene at temperatures for which no neutron diffraction experiments were available. H-atom nuclear quadrupole coupling constants derived from the resulting charge-density model were in good agreement with results obtained experimentally from spectroscopic measurements (Bürgi *et al.*, 2002).

The H-atom nuclear coupling constants derived from the charge density depend crucially on the model used for the H atoms, but the molecular quadrupole and dipole moments (Spackman, 1992; Spackman & Byrom, 1996; Roversi & Destro, 2004) are also sensitive to the model used for the H atoms. Parameters for the H atoms also affect most of the other properties of interest that are derived from the static electron density, *e.g.* intermolecular interaction energy (Espinosa *et al.*, 1998; Espinosa, Lecomte & Molins, 1999; Espinosa, Souhassou *et al.*, 1999; Spackman, 1999*a*,*b*) and electrostatic potentials (Stewart, 1991; Chen & Craven, 1995).

The topological analysis developed by Bader and co-workers (Bader, 1994) for theoretical electron densities is also extensively used for experimental crystal charge densities. It

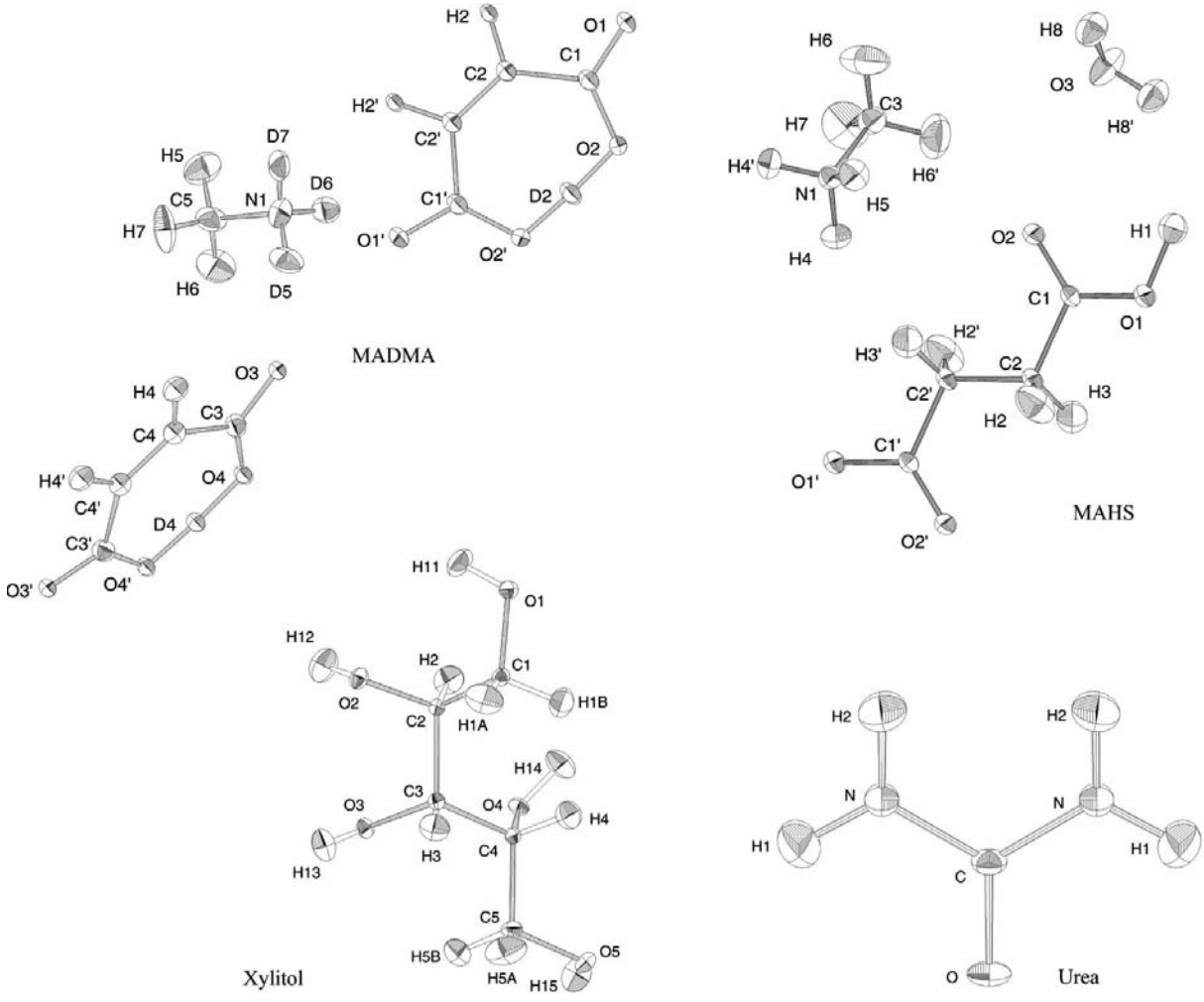

Figure 1
ORTEP plots (Johnson, 1976) of methylammonium hydrogen maleate (MADMA), methylammonium hydrogen succinate (MAHS), xylitol and urea. The plots of the four structures investigated are based on parameters derived from the neutron diffraction experiments. Ellipsoids are shown at the 50% probability level.

provides a powerful tool to characterize the interatomic interactions in molecular crystals through the properties of the bond or (3, −1) critical points. The bond critical points in the crystal electron density reflect both intra- and intermolecular interactions. Many intermolecular interactions in molecular crystals involve H atoms, and the models for H atoms employed in the charge-density refinements will have an impact on the characteristics of the bond critical points that involve H atoms.

Our recent neutron diffraction study of xylitol (Fig. 1) (Madsen *et al.*, 2003) provided accurate positional and thermal parameters for the H atoms. We have supplemented this study by measuring a highly redundant high-order and precise X-ray diffraction data set for xylitol at the same temperature. The different models used to generate parameters for the H atoms based exclusively on the X-ray data have been examined using the parameters derived from the neutron diffraction data set as a reference. Considering the increase in the number of experimental charge-density studies that include a topological analysis, we found it timely and important also to investigate how the models employed for the H atoms influence the topological properties of the resulting static electron densities.

Based on the analysis of the xylitol data, we were able to propose a relatively simple procedure to derive anisotropic thermal parameters for the H atoms that provides static electron densities that are virtually identical to those obtained using the neutron parameters. The general applicability of this procedure that provides reliable parameters for H atoms, when neutron data are unavailable, was examined by applying it to three other systems where both X-ray and neutron diffraction data are available; methylammonium hydrogen succinate monohydrate (MAHS, Flensburg *et al.*, 1995), methylammonium hydrogen maleate (MADMA, Madsen *et al.*, 1998) and urea (Birkedal *et al.*, 2004). *ORTEP* (Johnson, 1976) drawings of the compounds are shown in Fig. 1. Our analysis of these systems showed that the proposed procedure is suitable to give parameters for H atoms of water, methyl, methylene, methane, hydroxy, amide and ammonium groups that are in good agreement with the values from the neutron study, and thus give charge-density models virtually identical to those obtained with H-atom parameters from neutron data.

2. Experimental

Xylitol, purchased from Sigma, was recrystallized by evaporation of a 95% ethanol solution at room temperature. The size of the crystals seems to be controlled by the rate of evaporation, *e.g.* slow evaporation leads to large crystals.

2.1. Data collection

Several crystals were tested in order to obtain one that would ensure accurate high-resolution X-ray data. The data were collected on an Enraf–Nonius CAD4 diffractometer using graphite-monochromated Mo $K\alpha$ radiation. The temperature was controlled with an Oxford Cryosystems N_2 gas flow low-temperature device adjusted to 122.4 K by the phase transition of KH_2PO_4. Data were collected using $\omega - 2\theta$ scans up to $\sin\theta/\lambda = 1.2$ Å^{-1}. For every 600 reflections, the orientation of the crystal was checked by measuring the setting angles of 7 reflections, and 5 standard reflections were measured every 2.7 h. Details of the data collection are summarized in Table 1.[1]

Table 1
Data collection and processing for xylitol.

Crystal data	
Formula	$C_5H_{12}O_5$
Crystal system	Orthorhombic
Space group	$P2_12_12_1$
Unit-cell dimensions a, b, c [Å]	8.264 (5), 8.901 (2), 8.922 (2)
Volume [Å^3]	656.1 (4)
Z	4
Crystal colour	Colourless
Crystal size [mm]	0.26×0.32×0.37
Crystal description	Prism
Calculated density [g cm^{-3}]	1.540
Melting point [K]	366–368
Experimental conditions	
Wavelength (graphite monochromator) [Å]	0.71073
Temperature [K]	122.4 (5)
Data collection	
Reflections collected	44234
Data extending to $(\sin\theta/\lambda)_{max}$ [Å^{-1}]	1.2
Overall completeness	100%
Standard reflections	5
Cell determination reflections	20
Miller index limit of measurements: h / k / l	±20 / ±21 / ±21
Scan type	$\omega - 2\theta$
Scan range [°]	1.5 + 0.35 tanθ
Aperture size [mm]	4
Data with $I \geq 3\sigma(I)$ in 1.050 ≥ sinθ/λ ≥ 1.100 Å^{-1} shell	77%
Integration/merging	
Reflections merged	33102
Unique reflections (point group 222)	7320
R_{int} ($\sin\theta/\lambda \leq 1.1$ Å^{-1})	0.0171
Absorption corr. method	None
Linear absorption coefficient [mm^{-1}]	0.14
Scale correction min/max	0.943/1.052

2.2. Data reduction

The *DREAR* (Blessing, 1987) program package was used for the data reduction and data error analysis. The data were corrected for background, Lorentz and polarization effects. The intensities of the standard reflections decreased by 10% during the eight-week-long data collection. A correction for the decrease was made using a third-order polynomial fitted to the variation of the intensity of the standard reflections with time. The applied correction factors were in the range 0.943 to 1.052. The linear absorption coefficient is 0.14 mm^{-1} and, since the ratio between the maximal and minimal transmission factors was estimated to be 0.985, no absorption correction was considered necessary.

[1] Supplementary data, including a CIF file and structure factors for xylitol, and BCPs and H-atom nuclear coordinates for xylitol, MAHS, MADMA and urea, are available from the IUCr electronic archives (Reference: SH5011). Services for accessing these data are described at the back of the journal.

Table 2
Fractional atomic coordinates and anisotropic displacement parameters (10^2 Å^2) for C and O atoms in xylitol.

First row: neutron experiment. Second row: reference multipole model

	x	*y*	*z*	U^{11}	U^{22}	U^{33}	U^{12}	U^{13}	U^{23}
O1	0.67826 (10)	0.22884 (10)	0.42178 (9)	0.86 (3)	1.38 (4)	0.73 (3)	0.10 (3)	−0.03 (3)	0.03 (3)
	0.678540 (17)	0.228780 (17)	0.421700 (15)	0.946 (4)	1.627 (4)	0.997 (3)	0.067 (5)	−0.081 (4)	0.064 (4)
O2	0.61461 (10)	0.43594 (10)	0.18273 (10)	0.97 (3)	1.18 (3)	0.86 (3)	−0.32 (3)	−0.03 (3)	−0.07 (3)
	0.614850 (16)	0.436080 (17)	0.182510 (16)	1.079 (4)	1.418 (4)	1.141 (3)	−0.311 (4)	0.084 (4)	−0.058 (4)
O3	0.31823 (11)	0.43108 (10)	0.04011 (10)	1.19 (3)	1.03 (3)	0.65 (3)	0.04 (3)	−0.01 (3)	0.06 (3)
	0.318080 (18)	0.431130 (16)	0.040080 (14)	1.331 (4)	1.242 (4)	0.941 (3)	0.055 (4)	−0.058 (3)	0.053 (4)
O4	0.22887 (10)	0.12960 (10)	0.10839 (10)	1.01 (3)	0.91 (3)	0.97 (3)	0.16 (3)	−0.20 (3)	−0.15 (3)
	0.229080 (17)	0.129520 (16)	0.108450 (16)	1.202 (4)	1.104 (3)	1.144 (3)	0.173 (4)	−0.160 (4)	−0.167 (4)
O5	−0.08866 (10)	0.20517 (11)	0.21646 (10)	0.80 (3)	1.54 (4)	1.08 (3)	−0.15 (3)	0.16 (3)	−0.16 (3)
	−0.088770 (16)	0.204990 (18)	0.216170 (17)	0.921 (4)	1.774 (4)	1.281 (4)	−0.177 (5)	0.148 (4)	−0.174 (4)
C1	0.52470 (9)	0.29389 (9)	0.39045 (8)	0.79 (2)	1.28 (3)	0.68 (2)	0.02 (2)	0.04 (2)	−0.00 (2)
	0.524620 (15)	0.293750 (15)	0.390610 (14)	0.931 (4)	1.576 (3)	0.890 (3)	0.041 (5)	0.020 (4)	−0.037 (4)
C2	0.50050 (8)	0.32283 (8)	0.22439 (7)	0.77 (2)	0.83 (2)	0.62 (2)	−0.01 (2)	−0.01 (2)	−0.12 (2)
	0.500690 (14)	0.322920 (14)	0.224410 (13)	0.833 (3)	1.155 (3)	0.866 (3)	−0.036 (4)	−0.018 (3)	−0.099 (3)
C3	0.32774 (8)	0.37534 (8)	0.18980 (8)	0.72 (2)	0.85 (2)	0.76 (2)	0.04 (2)	−0.02 (2)	−0.09 (2)
	0.327690 (14)	0.375440 (14)	0.189850 (13)	0.876 (4)	1.118 (3)	0.882 (3)	0.024 (4)	−0.016 (3)	−0.102 (3)
C4	0.20081 (8)	0.25179 (8)	0.20983 (8)	0.68 (2)	0.97 (3)	0.60 (2)	0.01 (2)	−0.06 (2)	−0.08 (2)
	0.200820 (13)	0.251700 (13)	0.210040 (13)	0.827 (3)	1.189 (3)	0.879 (3)	0.019 (4)	−0.029 (3)	−0.056 (4)
C5	0.03186 (8)	0.31486 (9)	0.18585 (9)	0.73 (2)	1.05 (3)	1.25 (3)	0.10 (2)	−0.01 (2)	−0.13 (2)
	0.031830 (14)	0.314770 (15)	0.185570 (16)	0.872 (4)	1.276 (3)	1.514 (3)	0.085 (4)	−0.010 (4)	−0.149 (5)

Although data up to $\sin\theta/\lambda = 1.2$ Å^{-1} were collected, it was decided only to use the data extending to 1.1 Å^{-1} because $R_{\rm int}$ for the data in the range $1.1 \leq \sin\theta/\lambda \leq 1.2$ Å^{-1} exceeded 10%. This improved the merging of symmetry-equivalent reflections and refinement statistics significantly, with negligible effect on the multipole model parameters of the final model. A *SHELXL* (Sheldrick, 1997) refinement showed that the absolute configuration was in accordance with the known chemical structure of xylitol [the Flack parameter (Flack, 1983) was 0.0 (2)], therefore reflections were merged according to the crystal class in point group 222 with a resulting $R_{\rm int}$ of 0.0171. Further details of the data reduction are contained in Table 1.

2.3. Xylitol reference multipole model

The program *VALRAY* (Stewart *et al.*, 1998) was used for all the refinements of the structure and multipole parameters. The multipole expansion was extended up to the octopole level for the C and O atoms, and up to the quadrupole level for the H atoms. No local symmetry constraints were imposed on any of the pseudoatoms. The C- and O-atom core monopole populations were constrained to be equal. The set-up of radial functions in the multipole expansion is similar to the one described by Flensburg *et al.* (1995): for the lower multipoles ($l \leq 2$) on C and O atoms, the radial functions are density-localized (van der Wal & Stewart, 1984) orbital products of self-consistent-field (SCF) energy-optimized atomic orbitals in the basis of Clementi & Roetti (1974). For the octopoles and all multipoles on H atoms, single Slater-type functions were used [$r^n \exp(-\alpha r)$ with $n = 1, 2, 3$ for the dipole, quadrupole and octopoles, respectively]. For the C atoms, a common radial expansion/contraction parameter for the valence monopole, dipole and quadrupole level was refined, as was a common radial parameter for the octopoles of C atoms. An identical set-up was used for O atoms. Dispersion corrections to the C- and O-atom form factors corresponding to Mo $K\alpha$ radiation were taken from *International Tables for Crystallography*, Vol. C (Wilson & Prince, 1999). The radial expansion/contraction of the H atoms bound to O and C atoms was treated separately with a common radial parameter for the mono-, di- and quadrupole. The positions of the H atoms were taken from the neutron diffraction study. The positional parameters for the C and O atoms obtained in this refinement are virtually identical to the values obtained from the neutron diffraction study (Table 2).

Following the procedure described by Flensburg *et al.* (1995), Fig. 2 illustrates the comparison of the eigenvalues of the C and O atom mean square displacement (MSD) matrices of the two sets of ADPs. The direction cosines of the eigen-

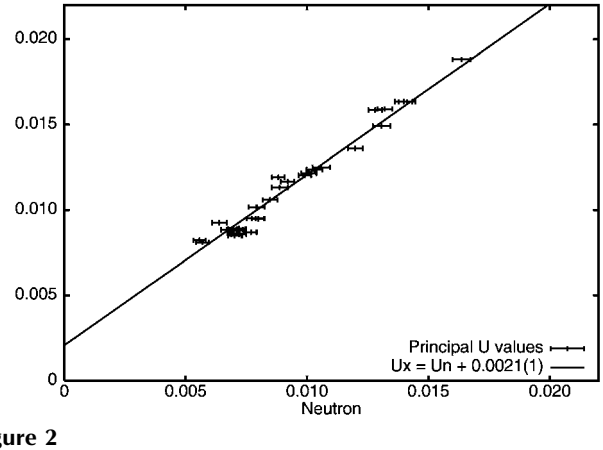

Figure 2
Principal components of the MSD matrices for the non-H atoms obtained from neutron and X-ray data [10^{-2} Å^2]. The line represents the least-squares fit. The error bars represent the s.u.s from the neutron experiment.

Table 3
Nuclear coordinates and anisotropic displacement parameters (10^2 Å^2) for H atoms in xylitol.

First row: ADPs with standard uncertainties, derived from the neutron diffraction data and adjusted according to the difference between the C- and O-atom ADPs from neutron and X-ray experiments. Second row: best anisotropic model based on addition of rigid-body motion and internal vibrations.

	x	y	z	U^{11}	U^{22}	U^{33}	U^{12}	U^{13}	U^{23}
H1*A*	0.5127 (2)	0.4016 (2)	0.4520 (2)	3.36 (8)	2.74 (8)	2.63 (8)	0.81 (7)	−0.24 (8)	−1.12 (7)
	0.50798	0.39938	0.45033	3.00	2.58	2.43	0.31	−0.32	−0.89
H1*B*	0.4318 (2)	0.2168 (3)	0.4333 (2)	2.05 (7)	3.99 (10)	2.83 (8)	−0.70 (7)	0.18 (6)	1.23 (8)
	0.43265	0.21696	0.43449	2.10	3.23	2.62	−0.73	0.03	0.76
H2	0.5262 (2)	0.21900 (20)	0.16109 (20)	2.10 (6)	2.02 (6)	2.64 (7)	0.13 (6)	0.11 (6)	−0.72 (6)
	0.52363	0.22002	0.15977	2.34	2.07	2.14	0.24	0.18	−0.55
H3	0.2979 (2)	0.46794 (19)	0.26822 (19)	2.47 (7)	1.96 (6)	2.24 (7)	0.23 (6)	−0.04 (6)	−0.66 (6)
	0.29706	0.46475	0.27006	2.45	2.09	2.24	0.24	0.10	−0.70
H4	0.2073 (2)	0.2095 (2)	0.32600 (18)	2.50 (7)	2.87 (8)	1.60 (6)	−0.04 (6)	−0.08 (6)	0.48 (6)
	0.20526	0.20557	0.32433	2.42	2.75	1.58	−0.07	0.01	0.31
H5*B*	0.0197 (2)	0.3565 (2)	0.0695 (2)	2.48 (7)	3.25 (9)	2.85 (8)	−0.01 (7)	−0.53 (7)	1.12 (7)
	0.02139	0.35452	0.07045	2.54	3.44	2.06	0.02	−0.36	0.46
H5*A*	0.0131 (2)	0.4103 (2)	0.2618 (3)	2.61 (8)	2.67 (8)	4.78 (11)	0.24 (7)	0.37 (8)	−1.81 (8)
	0.00640	0.40631	0.26338	2.40	2.89	3.19	0.21	0.16	−1.41
H11	0.75601 (20)	0.2432 (2)	0.33761 (20)	1.81 (6)	3.17 (8)	2.13 (7)	−0.12 (6)	0.45 (6)	0.34 (7)
	0.74973	0.23857	0.33675	1.79	3.34	2.03	0.27	0.32	0.20
H12	0.6521 (2)	0.4163 (2)	0.0805 (2)	2.85 (8)	3.02 (8)	2.19 (8)	−0.47 (7)	0.70 (6)	−0.19 (7)
	0.65817	0.41540	0.08458	2.54	3.09	1.71	−0.55	0.54	−0.19
H13	0.3268 (2)	0.54153 (19)	0.0450 (2)	3.18 (8)	1.76 (6)	2.28 (7)	−0.10 (6)	0.10 (7)	0.23 (6)
	0.32826	0.53868	0.04827	3.27	1.72	2.50	−0.19	−0.31	0.21
H14	0.2766 (2)	0.04897 (20)	0.1667 (2)	3.34 (8)	1.95 (7)	2.78 (8)	0.86 (7)	−0.30 (7)	0.14 (6)
	0.27946	0.05176	0.16722	2.76	1.90	2.27	0.46	−0.45	0.11
H15	−0.1183 (2)	0.1568 (2)	0.1209 (2)	2.75 (8)	2.79 (8)	2.26 (7)	−0.64 (7)	0.02 (6)	−0.70 (7)
	−0.12210	0.15814	0.12389	2.40	2.89	2.21	−0.55	−0.20	−0.44

vectors of the MSD matrices are in good agreement except for a few cases where two eigenvalues are virtually identical, allowing small errors in the ADPs to cause rather large changes in the direction of the eigenvectors. The two sets of eigenvalues are related by the equation $U_{\text{X-ray}} = U_{\text{neutron}} + 0.0021$ Å^2, indicating that the discrepancy is not due to difference in temperature between the experiments. In this case, the relation would have been multiplicative. Differences of this order of magnitude are not uncommon (Blessing, 1995) and may be caused by lack of correction of thermal diffuse scattering or insufficient extinction correction of the neutron diffraction experiment. Part of the discrepancy can be attributed to the spectral truncation. In an investigation of $NiSO_4{\cdot}H_2O$, Rousseau *et al.* (2000) reported a truncational component to the temperature factor of 0.00063 Å^2 for graphite-monochromated sealed-tube Mo radiation operating at 50 kV, thus closely resembling the set-up used in this study.

The parameters for the H atoms obtained in the neutron diffraction experiment were adjusted according to this difference and used as fixed parameters in the multipole refinement with respect to the X-ray data, providing the final reference model. The positional and thermal parameters for the H atoms are listed in Table 3.

The quantity minimized in all refinements was $\varepsilon = \sum w(|F_o|^2 - |F_c|^2)^2$ with weights $w = 1/\sigma^2(F_o^2)$ based on counting statistics and the sum extending over all measured reflections. To ensure that a true minimum was found with reliable estimates of the variances of the refined parameters and derived properties, the final cycles of the refinements of the 366 parameters included full second derivatives in the least-squares matrix (Stewart *et al.*, 1998). The refinement

Table 4
Refinement statistics for xylitol models refined against X-ray data.

Model	$R(F^2)$	$wR(F^2)$	GOF	Parameters
IAM	0.0369	0.0529	1.4042	140
HIGH	0.0244	0.0349	0.609	140
POL	0.0365	0.0535	1.4218	140
ISO:I	0.0369	0.0529	1.4042	140
ISO:II	0.0366	0.0525	1.3944	140
Reference	0.0149	0.0240	0.6468	366
Best isotropic	0.0159	0.0247	0.6666	364
Best anisotropic	0.0149	0.0239	0.6462	366

statistics for this reference model are listed in Table 4. Plots of the residual density (using all data) in planes through the xylitol molecule are featureless. The standard uncertainty of the residual density is around 0.05 e Å^{-3} and none of the peaks in the residual density exceed three s.u.s. A full topological analysis of the static charge density based on this reference model revealed three minima for which the electron density is slightly negative, the most negative being −0.006 (3) e Å^{-3}.

3. Estimates of H-atom nuclear positions

Four commonly used procedures to obtain nuclear positions for H atoms have been compared with the values from the reference model. An overview of the different models is presented in the first part of Table 5.

IAM: *IAM refinement*. Standard IAM (independent-atom model) refinement using *SHELXL* (Sheldrick, 1997)

Table 5
Description of xylitol models.

R: refined parameters; **E**: estimated parameters; **N**: derived from neutron diffraction experiment.

	C and O atoms			H atoms				
Model	*xyz*	ADPs	Multipoles	*xyz*	ADPs	U_{iso}	Multipoles	Treatment of H atoms
Reference model	**R**	**R**	**R**	**N**	**N**		**R**	H-atom positions and ADPs (adjusted) from neutron diffraction study
IAM	**R**	**R**		**R**		**R**		SDS H-atom scattering factor (Stewart *et al.*, 1965)
HIGH	**R**	**R**		**R**		**R**		Data: $\sin(\theta)/\lambda \geq 0.77$ Å^{-1}
POL	**R**	**R**		**R**		**R**		Polarized scattering factor for H atoms
IDEAL	**IAM**	**IAM**		**E**		**IAM**		*X*—H bond lengths extended to idealized values
ISO:I	**R**	**R**		**R**		**R**		H-atom scattering factor: single STF, exponent 2.32 bohr^{-1}.
ISO:II	**R**	**R**		**R**		**R**		H-atom scattering factor: single STF, exponent 2.48 bohr^{-1}
Best isotropic	**R**	**R**	**R**	**E**	**E**		**R**	H-atom coordinates from IDEAL. H-atom U_{iso} from ISO:I
Best anisotropic	**R**	**R**	**R**	**E**	**E**		**R**	H-atom coordinates from IDEAL. H-atom ADPs from TLS:mean (§4.2)

employing H-atom scattering factors from Stewart *et al.* (1965) (SDS).

IDEAL: *idealized positions*. The C—H and O—H bond lengths from the IAM refinement were elongated to match mean bond lengths from neutron diffraction studies listed in *International Tables for Crystallography*, Vol. C (Allen *et al.*, 1999). This elongation did not involve a refinement of nuclear parameters.

HIGH: *high-angle refinement*. A range of high-angle refinements was conducted where data with scattering angles below a selected cut-off value were excluded from the least-squares sums. The results presented here are based on a refinement with a cut-off value of 0.77 Å^{-1} in $\sin\theta/\lambda$, which provided the best agreement with the neutron parameters.

POL: *polarized H atom*. Polarized density function with a bond-directed dipole. A similar procedure has recently been used by Roversi & Destro (2004). The dipole used was the average of the refined H-atom dipole parameters from the combined neutron and X-ray experimental charge-density studies of the MAHS, MADMA, xylitol and urea reference models (see §6). For the H(C) bound to a C atom, a dipole population of 0.45 e Å and α exponent for the exponential-type radial function of 2.42 bohr^{-1} was employed. For H(O), the equivalent parameters were dipole population 0.46 e Å and α = 2.56 bohr^{-1}.

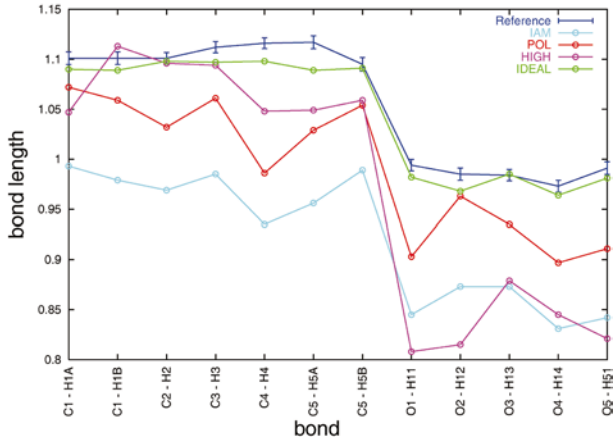

Figure 3
Estimates of *X*—H bond lengths [Å] for xylitol. Error bars shown for the reference model are the s.u.s obtained from the neutron experiment.

In comparison to the reference (neutron diffraction) model, none of the four models shows any significant deviation of the direction of the *X*—H bond; the root mean square (r.m.s.) deviation of the direction of the *X*—H bond vectors is 2.1 (1.2)°, so the comparison can be limited to *X*—H bond lengths. Fig. 3 illustrates the *X*—H bond lengths in xylitol as obtained by the different models. IAM, POL and HIGH all show large discrepancies in the positions of the H atoms. Not unexpectedly, the IDEAL model derived from neutron data provides the best agreement with our reference model, which is a demonstration of the agreement between the *X*—H bond lengths in xylitol and the values from other neutron studies.

It appears that the usual practice of extending the bond lengths to idealized values gives H-atom positions that are in agreement with the reference model for xylitol. The mean deviation from the neutron result is 0.012 (8) Å in *bond lengths*, which corresponds to a mean deviation in *positions* of 0.041 (19) Å.

4. Estimates of H-atom displacement parameters

The next step was to investigate the different models that can be employed to obtain displacement parameters for the H atoms from X-ray diffraction data. An overview of the different models we have examined is given in Table 5. In this section, we focus first on the commonly used isotropic description and secondly on the methods to derive anisotropic displacement parameters.

4.1. Isotropic description

The isotropic displacement parameters obtained from the independent-atom model (IAM) depend strongly on the H-atom form factor employed in the refinement against the X-ray data. Most refinement programs like *SHELXL* (Sheldrick, 1997) have the SDS (Stewart *et al.*, 1965) form factor as the default option. It is based on a fit to the form factor of the H_2 molecule obtained from *ab initio* calculations. Compared

with the form factor of an isolated H atom, it corresponds to a contraction of the electron density. In the *VALRAY* program system (Stewart *et al.*, 1998), the SDS form factor is represented by the Fourier–Bessel transform of a single exponential type function $\exp(-\alpha r)$ with α exponent of 2.32 bohr^{-1}. The model referred to as ISO:I used this form factor. The resulting H-atom parameters are identical to those obtained by a *SHELXL* refinement.

The electron density of the H atom may be even further contracted when bound to electronegative elements like C, N and O (Stewart, 1976; Coppens *et al.*, 1979). We have therefore examined the model where the exponent α in the single exponential type function is increased to 2.48 bohr^{-1} (Hehre *et al.*, 1969), referred to as ISO:II. The positions of the H pseudoatoms were allowed to relax in these two IAM refinements giving rise to the apparent shortening of the X—H bonds illustrated in Fig. 3. The two models give R values similar to the one obtained from the IAM (*SHELXL*) refinement that employs the SDS form factor (Stewart *et al.*, 1965).

For comparison, we conducted a least-squares refinement against the neutron data using a model with *isotropic H-atom displacement parameters*. The resulting isotropic displacement parameters were subsequently adjusted to allow for the systematic discrepancy ($U_{\text{X-ray}} = U_{\text{neutron}} + 0.0021$ Å^2) between the neutron and X-ray non-H-atom ADPs. These parameters should represent the 'best isotropic' model, and are given as model ISO:NEUT in Table 6.

The isotropic displacement parameters obtained from the two different H-atom scattering models ISO:I and ISO:II differ internally and show great discrepancies from the 'best isotropic' model ISO:NEUT. Refinement of the isotropic displacement parameters while fixing the H-atom positions to the neutron diffraction values only increased the discrepancies. It is evident that the isotropic displacement parameters are very sensitive to the choice of α exponent. To obtain values close to the neutron diffraction parameters would obviously require *ad hoc* adjustment of the α exponent for the H atoms.

4.2. Anisotropic description

Previous analyses of the ADPs for H atoms obtained by neutron diffraction (Johnson, 1970; Weber *et al.*, 1991; Gao *et al.*, 1994; Luo *et al.*, 1996; Madsen *et al.*, 2003) have indicated that the combined use of rigid-body displacements obtained from the framework of non-H atoms and estimates of the H-atom internal motion can give reasonable estimates of the H-atom ADPs. A direct comparison between the ADPs for H atoms derived with this approach originally proposed by Hirshfeld (1976) and those obtained from neutron diffraction data has not been conducted previously, and we found it worthwhile to pursue this aspect. The analysis is based on the assumption that the rigid-body and internal motions are uncorrelated, and the total atomic mean square displacement matrix can be obtained as a sum of the two contributions:

$$U^{ij} = U^{ij}_{\text{rigid}} + U^{ij}_{\text{internal}}. \qquad (1)$$

Table 6
Isotropic displacement parameters [10^{-5} Å^2] for the H atoms in xylitol based on two isotropic refinements against X-ray data (ISO:I and ISO:II) and the refined isotropic parameters against neutron data (ISO:NEUT).

Atom	ISO:I	ISO:II	ISO:NEUT
H1*A*	156 (10)	248 (10)	262 (5)
H1*B*	166 (10)	252 (10)	251 (5)
H2	152 (9)	229 (9)	192 (4)
H3	124 (9)	209 (9)	200 (4)
H4	185 (10)	273 (10)	208 (4)
H5*B*	160 (10)	247 (10)	259 (5)
H5*A*	202 (10)	304 (11)	290 (5)
H11	346 (14)	472 (15)	209 (4)
H12	322 (13)	428 (14)	247 (5)
H13	422 (16)	550 (17)	218 (4)
H14	303 (13)	420 (14)	241 (5)
H15	326 (14)	436 (14)	237 (5)

The internal vibrations can in principle be obtained from semi-empirical or *ab initio* calculations, but our efforts along these lines for xylitol using single-molecule Hartree–Fock and density-functional-theory calculations gave internal mean square displacements (MSDs) larger than the total MSDs obtained from the diffraction experiments, presumably because the isolated xylitol molecule has a very flat potential-energy surface (Madsen *et al.*, 2003). Instead, we obtained the internal mode contribution from an analysis of ADPs derived from neutron diffraction data (Madsen *et al.*, 2003). The sum of the contributions from the different internal vibrational modes comprises the total internal motion. If the internal mode k has a MSD $\langle u^2\rangle_k$ in the direction given by the unit vector $\mathbf{e}_k$, then the total atomic internal motion is

$$U^{ij}_{\text{internal}} = \sum_k \langle u^2\rangle_k \mathbf{e}_k \mathbf{e}_k^T, \qquad (2)$$

where $\mathbf{e}_k^T$ is the transpose of $\mathbf{e}_k$, expressed in an orthonormal coordinate system. In case the atomic coordinates are expressed in an oblique crystal coordinate system, a transformation to an orthonormal system must be performed in order to calculate the $\mathbf{e}_k$ unit vectors. The atomic MSD matrix resulting from this analysis must be transformed back to the (oblique) crystal system.

Information about the total internal motion can be provided from the analysis of ADPs from neutron diffraction data. The internal motion can be decomposed along three directions corresponding to bond stretch vibration, as well as two orthogonal vibrations in the plane perpendicular to the X—H interatomic axis (Madsen *et al.*, 2003).

A preliminary multipole refinement with hydrogen nuclear parameters fixed at values obtained by a standard IAM refinement gave ADPs for non-H atoms that were almost identical to those of the reference model (Table 2). The differences between the sets of ADPs are around 0.0001 Å^2. A **TLS** analysis using the *THMA11* program (Schomaker & Trueblood, 1998) of these ADPs showed that they were described reasonably well by the rigid-body motion [$wR(U^{ij}) = 0.095$].

Table 7
Mean square amplitudes in units of 10^{-4} Å^2 for internal vibrations of H nuclei taken from Madsen *et al.* (2003).

	No. of X—H groups	X—H stretch	X—X—H out-of-plane	X—X—H in-plane	$U_{iso} - U_{bond}$
Methylene	18	51 (11)	145 (33)	246 (72)	86 (32)
Methyl	14	38 (13)	369 (90)	245 (115)	134 (34)
Methine	28	50 (13)	148 (27)	140 (23)	79 (31)
Hydroxy	24	35 (22)	183 (43)	101 (34)	67 (18)
Water	7	54 (27)	174 (70)	157 (74)	85 (17)
Ammonium	5	28 (15)	150 (33)	141 (50)	70 (15)

Four different models used to obtain anisotropic displacement parameters for the H atoms were compared with the reference model:

TLS. The H-atom ADPs were obtained solely from the rigid-body motion of the non-H atoms.

TLS:crude. The displacements from the rigid-body motion were combined with a crude estimate of the internal motion. We have chosen a common bond-directed MSD for all H atoms of 0.005 Å^2 corresponding to the mean value from all X—H bonds investigated by Madsen *et al.* (2003), and 0.020 Å^2 in the directions perpendicular to the bond.

TLS:mean. The **TLS** rigid-body motion was combined with an estimate of in-plane and out-of-plane internal vibrations based on mean values derived from the analysis of neutron diffraction studies (Madsen *et al.*, 2003). The values used are listed in Table 7 for the out-of-plane and in-plane vibrations; the bond-directed MSD was 0.005 Å^2 .

RIDING:mean. Finally, a simple riding model was tested. The H atoms were assigned the same MSD as the atom they are bonded to, in addition to similar internal motion as in model TLS:mean.

The overall agreement between the estimates and the reference model is reflected in the R factor,

$$R(U^{ij}) = \frac{\sum_{i,j} |U^{ij}_{\rm est} - U^{ij}_{\rm ref}|}{\sum_{i,j} |U^{ij}_{\rm ref}|},$$

where $U^{ij}_{\rm ref}$ and $U^{ij}_{\rm est}$ are the ADPs of the reference and estimated model, respectively. For the TLS:mean model, the agreement factor is 14%, whereas TLS:crude and RIDING:mean have agreement factors of 21 and 17%, respectively. All three models are acceptable, whereas model TLS has an agreement factor of 65%.

TLS:mean evidently provides the best overall agreement with the reference model derived from the neutron experiment. The displacement parameters resulting from these two models[2] are listed in Table 3.

The mean difference between the parameters is 0.002 Å^2 with a standard deviation of 0.002 Å^2. Here it is worth remembering that the standard uncertainties derived from the neutron diffraction study are around 0.0007 Å^2.

Further indication of the general agreement between estimated and neutron-diffraction-derived ADPs is warranted from the previous work in which an estimate of the internal vibrations is obtained by subtracting the (**TLS**) rigid-body motion from the total H-atom ADPs from neutron diffraction (Johnson, 1970; Weber *et al.*, 1991; Gao *et al.*, 1994; Luo *et al.*, 1996; Madsen *et al.*, 2003).

The analysis of mean values of the internal vibrations found by Madsen *et al.* (2003) revealed a bond-directed internal MSD in all X—H bonds of 0.005 Å^2 with a r.m.s. deviation of 0.002 Å^2, whereas the in-plane displacements of CH_2 groups have a r.m.s. deviation of 0.007 Å^2. The precision of the estimated internal MSD appears to have a strong dependence on the direction and chemical environment. Table 7 indicates that the bond-directed MSDs are best defined, which is important since most of the electron density associated with the H atom is polarized into the bond direction.

5. Topological analysis of static electron densities derived from different H-atom models

The topological analysis developed by Bader and co-workers (Bader, 1994) for theoretical electron densities identifies critical points $[\nabla\rho(r_c) = 0]$ in the electron density. The so-called bond or $(3, -1)$ critical points (BCP) are particularly interesting from a chemical point of view. Their second-derivative matrix has two negative and one positive eigenvalues, and they are localized on interatomic interaction lines. The position (r_c) and associated values of the electron density $\rho(r_c)$ and the Laplacian $\nabla^2\rho(r_c)$ (sum of eigenvalues of the second-derivative matrix) are used as quantitative measures to characterize the interatomic interactions. The topological analysis is also extensively used for experimental crystal densities. Therefore, we found it important to investigate how the different approaches used to model the H atoms described in the previous paragraphs influence the characteristics of the BCPs in experimental electron densities. We have conducted multipole refinements (resembling the reference model in terms of electronic parameters) for models used to obtain parameters for the H atom described in §4.2. The positional parameters were those obtained by extension to idealized neutron values (IDEAL), they were used in connection with different H-atom scattering factors employed in refinements of isotropic displacement parameters (ISO:I, ISO:II). We found that the characteristics of the BCP differ significantly from those obtained with the reference model. Similar discrepancies were observed using the density optimized radial exponents by Volkov *et al.* (2001). The best isotropic model is the one combining IDEAL

[2] Tables comparing the remaining models with the reference model are found in the supplementary material. See deposition footnote.

Table 8
Key experimental figures for MAHS, MADMA and urea.

	MAHS		MADMA		Urea	
	X-ray	Neutron	X-ray	Neutron	X-ray	Neutron
Wavelength [Å]	0.71073	1.013	0.71073	1.047	0.5996 (1)	1.0791 (2)
Monochromator	Graphite	Be(002)	Graphite	Be(002)	Si(111)	Ge(220)
Temperature [K]	110	≥110	122.4 (5)	122.4 (5)	123 (2)	123
Reflections collected	28158	2484	31455	2958	3942	342
Unique reflections	6147	2094	7192	2067	1045	342
Data extending to $\sin(\theta)/\lambda$ [Å^{-1}]	1.2176	0.6995	1.08	0.73	1.44	0.77
$R_{\rm int}$	0.013	0.015	0.0246	0.0137	0.0141	0.02

Table 9
Refinement statistics for MAHS, MADMA and urea models refined against X-ray data.

Structure	Model	$R(F^2)$	$wR(F^2)$	GOF	Parameters
MAHS	Reference	0.0208	0.0288	0.7332	280
	Best isotropic	0.0224	0.0306	0.7778	277
	Best anisotropic	0.0208	0.0290	0.7381	280
MADMA	Reference	0.0195	0.0298	1.1019	343
	Best isotropic	0.0219	0.0311	1.1527	342
	Best anisotropic	0.0198	0.0296	1.0960	343
Urea	Reference	0.0087	0.0110	1.1890	76
	Best isotropic	0.0084	0.0115	1.2484	75
	Best anisotropic	0.0086	0.0110	1.1967	76

with ISO:I, where the radial part of the H-atom form factor was kept at the standard molecular value of $\alpha = 2.48$ bohr^{-1}. The characteristics of the intramolecular BCP obtained with this model is shown in Fig. 4 together with the equivalent results from the reference model. The 'best isotropic' model shows systematic differences from the reference model, the values of the electron density are too small for the C—H and too large for the O—H bonds. It is noteworthy that the application of the 'best isotropic' model leads to systematically lower values of the Laplacian characterizing the bonds between non-H atoms.

The static electron densities calculated from the different models used to obtain anisotropic displacement parameters for the H atoms by combination of rigid-body motion and the internal vibrations (TLS:crude, TLS:mean and RIDING: mean) are in much better agreement with the electron density of the reference model than the one from the 'best isotropic' model. However, the TLS model provides an obviously poorer agreement than the other two models that include the contribution from internal vibrations. It is noteworthy that the RIDING:mean model does not differ significantly from the models based on the rigid-body analysis. The 'best anisotropic' model is obtained by combining positions from the IDEAL model with anisotropic displacement parameters from TLS:mean. The H-atom nuclear parameters for this model are given in Table 3. The results from the topological analysis based on this 'best anisotropic' model are shown in Fig. 4. The convincing agreement with the results based on the reference model demonstrates that it is possible to conduct a charge-density study with a topological analysis based exclusively on X-ray diffraction data for xylitol. The estimate of anisotropic ADPs combined with positions for the H atoms obtained by

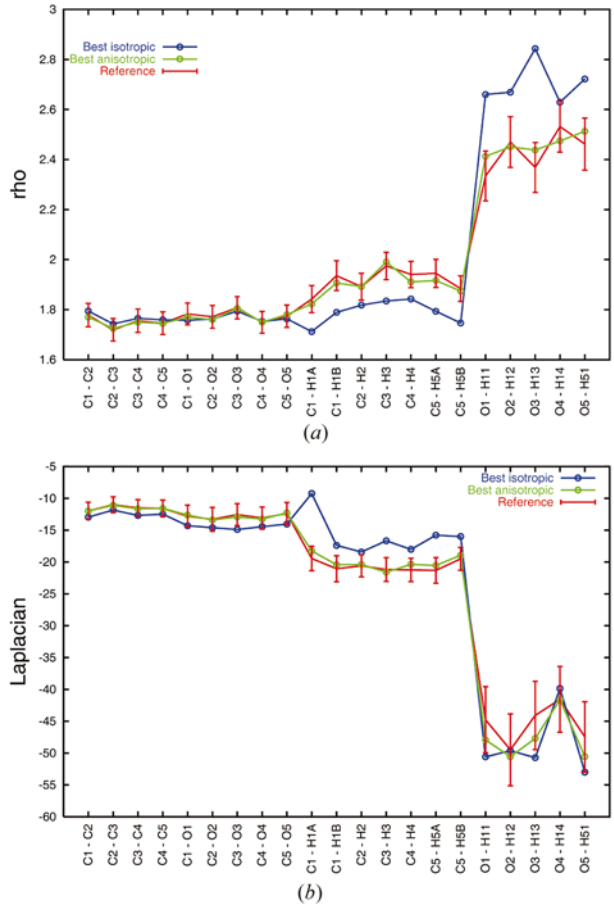

Figure 4
Electron density [e Å^{-3}] and Laplacian [e Å^{-5}] in the intramolecular BCPs of three xylitol models. The error bars correspond to three s.u.s of the properties of the reference model.

extending the X—H bond length to match bond lengths obtained from neutron diffraction is sufficient to provide a multipole model that is in good agreement with one obtained from the combined neutron and X-ray diffraction study. On the other hand, Fig. 4 provides strong evidence that the frequently used 'best isotropic' model is not capable of giving a static electron density with reliable topological properties.

6. Application to other systems: urea, MAHS and MADMA

We have examined if the 'best anisotropic' model is applicable to other systems by employing it on three other systems for which both accurate neutron and X-ray data are available: urea, methylammonium hydrogensuccinate monohydrate (MAHS) and methylammonium hydrogenmaleate

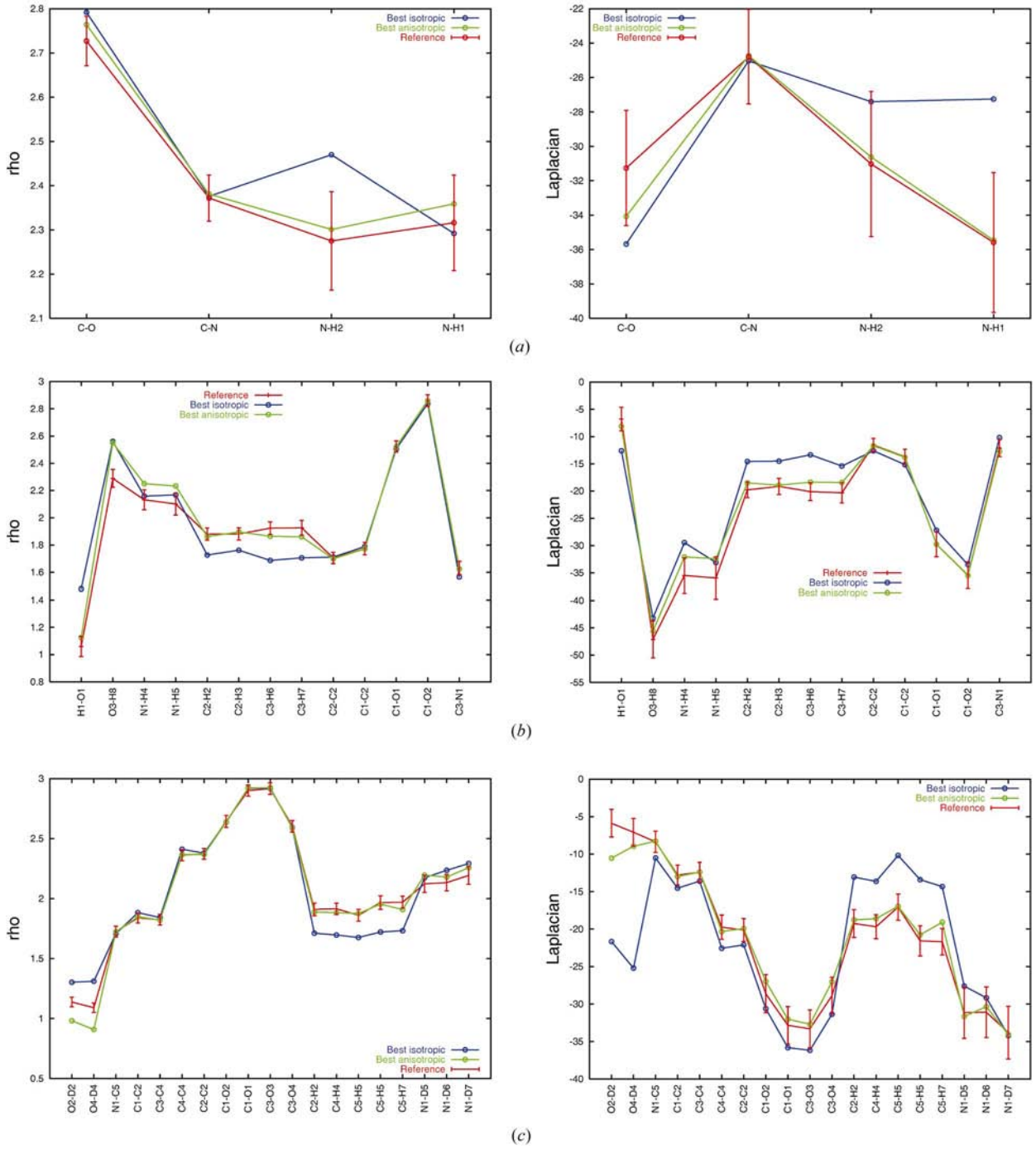

Figure 5
Electron density [e Å^{-3}] and Laplacian [e Å^{-5}] in the intramolecular BCPs of multipole models of (*a*) urea, (*b*) MAHS and (*c*) MADMA. The multipole models 'best isotropic' and 'best anisotropic' are compared to the reference models (red). Error bars correspond to three s.u.s.

(MADMA). Key experimental parameters for the three compounds are listed in Table 8. The procedures 'best isotropic' and 'best anisotropic' as described above for xylitol were used to obtain parameters for the H atoms in the three structures.[3] These were compared with the reference models based on the combined use of X-ray and neutron diffraction data. The reference models were taken from the original work (Flensburg *et al.*, 1995; Madsen *et al.*, 1998; Birkedal *et al.*, 2004). The anisotropic ADPs of the non-H atoms of the anions in MAHS and MADMA were subjected to a **TLS** analysis using the *THMA11* program (Schomaker & Trueblood, 1968). This resulted in a very satisfactory fit with $R_w(U^{ij})$ of 0.063 for MAHS and 0.021, 0.022 for the anions in MADMA. It is not possible to use a **TLS** model for the water molecule in MAHS and to refine a **TLS** model to the non-H atoms of the methylammonium ion in MAHS and MADMA. For the H atoms bonded to these moieties, we estimated their ADPs using the RIDING:mean model. The electronic parameters used in the reference models were also employed to obtain the multipole models and static electron densities for the 'best isotropic' and 'best anisotropic models'. The standard molecular value was used for the radial part of the H-atom form factor in the 'best isotropic' description. The refinement statistics obtained for the three systems are listed in Table 9.

6.1. Topological analysis

The characteristics of the intramolecular BCP obtained from topological analysis of the static electron densities from the 'reference', 'best isotropic' and 'best anisotropic' models are shown in Fig. 5. The results from urea, MAHS and MADMA generally confirm the results obtained from the analysis of xylitol. The topological analysis of the crystal electron densities showed that the 'best isotropic' model leads to results that are significantly different from the 'reference' model. The model used for the H atoms affects the entire static electron density as illustrated by the variation in the Laplacian of the BCP between the non-H atoms, the differences are even more pronounced than for xylitol. The properties of BCPs for C—O bonds show the largest differences. These polarized bonds are characterized by having a very steep Laplacian close to the BCP, which explains why small changes in the position of the BCP may have large effects on the Laplacian. An excellent agreement is found between the static electron densities from the 'reference' and 'best anisotropic' models for urea and the anions of MAHS and MADMA. Exceptions are the H atoms that are involved in the very short intramolecular O—H—O hydrogen bond in MADMA (D2 and D4). Larger differences are also seen for some of the H atoms of the methylammonium groups. These discrepancies seem to be due to the use of riding motion.

The assignment of a common bond-directed internal MSD of 0.005 Å^2 to all X—H bonds is based on the observation that the differences between C—H, N—H and O—H bonds are very small as indicated by spectroscopic measurements; typical stretching frequencies of O—H bonds are 3700 cm^{-1}, whereas aliphatic C—H bonds have values around 2850 cm^{-1}, corresponding to MSDs of 0.0048 and 0.0064 Å^2, respectively. For the H atoms in the short hydrogen bonds in MADMA, the relatively strong interatomic force constants should have been taken into account in the estimate of the bond-directed internal motion.

The treatment of H atoms affects the entire static electron density. The C—C, C—N and C—O BCPs are considerably affected when isotropic H-atom displacement parameters are used. A similar but smaller effect was seen for xylitol.

7. Conclusions

A range of approaches to estimate H-atom nuclear parameters in the absence of neutron diffraction data has been examined.

Estimation of H-atom positions based on extending the bond length to match typical values derived from neutron diffraction studies gives results in close accordance with the reference positions obtained by refinement with respect to neutron diffraction data.

The use of isotropic displacement parameters obtained by refinement with respect to the X-ray data leads to significant discrepancies in the static charge-density models compared to a reference model based on combined X-ray and neutron diffraction data.

It is important to stress that the isotropic model has a rather large effect on all the topological features, also those *not* involving the H atoms. Significant changes in the Laplacian as well as the electron density in the BCPs are seen in all the structures when isotropic ADPs are used for the H atoms. As a consequence, an improved description of the models for H-atom displacements is necessary for the study of properties intrinsic to the H atoms, as well as other molecular properties.

A comparative study of H-atom parameters from X-ray and neutron diffraction data for xylitol has validated a procedure that provides anisotropic displacement parameters for H atoms from X-ray diffraction data in agreement with the neutron results. It is based on estimation of anisotropic ADPs for H atoms as a sum of the rigid-body contribution from a **TLS** analysis of the ADPs of non-H atoms and an estimate of the internal motion from analysis of ADPs from a variety of structures obtained from neutron diffraction data. It represents a considerable improvement compared to the isotropic treatment and provides crystal charge densities that are almost indistinguishable from those making use of neutron diffraction results.

We are grateful for the valuable help from Flemming Hansen in the collection of the xylitol X-ray data. The research is supported by the Danish Natural Science Council. AØM is grateful to the European Synchrotron Radiation Facility for funding of his PhD studies.

[3] The resulting nuclear parameters for H atoms are given in the supplementary material along with the parameters from the reference models.

References

Allen, F. H., Watson, D. G., Brammer, L., Orpen, A. G. & Taylor, R. (1999). *International Tables for Crystallography*, Vol. C, edited by A. J. C. Wilson & E. Prince, pp. 782–803. Dordrect/Boston/London: Kluwer Academic Publishers.

Bader, R. F. W. (1994). *Atoms in Molecules.* Oxford University Press.

Birkedal, H., Madsen, D., Mathiesen, R., Knudsen, K., Weber, H.-P., Pattison, P. & Schwarzenbach, D. (2004). *Acta Cryst.* A**60**, 371–381.

Blessing, R. H. (1987). *Crystallogr. Rev.* **1**, 3–58.

Blessing, R. H. (1995). *Acta Cryst.* B**51**, 816–823.

Bürgi, H. B. & Capelli, S. C. (2000). *Acta Cryst.* A**56**, 403–412.

Bürgi, H.-B., Capelli, S. C., Goeta, A. E., Howard, J. A. K., Spackman, M. A. & Yufit, D. S. (2002). *Chem. Eur. J.* **8**, 3512–3521.

Capelli, S. C., Förtsch, M. & Bürgi, H. (2000). *Acta Cryst.* A**56**, 413–424.

Chen, L. & Craven, B. (1995). *Acta Cryst.* B**51**, 1081–1097.

Clementi, E. & Roetti, C. (1974). *At. Data Nucl. Data Tables*, **14**, 177–478.

Coppens, P., Guru Row, T. N., Leung, P., Stevens, E. D., Becker, P. J. & Yang, Y. W. (1979). *Acta Cryst.* A**35**, 63–72.

Destro, R. & Merati, F. (1995). *Acta Cryst.* B**51**, 559–570.

Eisenstein, M. & Hirshfeld, F. L. (1983). *Acta Cryst.* B**39**, 61–75.

Espinosa, E., Lecomte, C. & Molins, E. (1999). *J. Chem. Phys.* **300**, 745–748.

Espinosa, E., Molins, E. & Lecomte, C. (1998). *J. Chem. Phys.* **285**, 170–173.

Espinosa, E., Souhassou, M., Lachekar, H. & Lecomte, C. (1999). *Acta Cryst.* B**55**, 563–572.

Flack, H. D. (1983). *Acta Cryst.* A**39**, 876–881.

Flaig, R., Koritsanszky, T., Zobel, D. & Luger, P. (1998). *J. Am. Chem. Soc.* **120**, 2227–2238.

Flensburg, C., Larsen, S. & Stewart, R. F. (1995). *J. Phys. Chem.* **99**, 10130–10141.

Gao, Q., Weber, H.-P., Craven, B. M. & McMullan, R. K. (1994). *Acta Cryst.* B**50**, 695–703.

Harel, M. & Hirshfeld, F. L. (1975). *Acta Cryst.* B**31**, 162–172.

Hehre, W. J., Stewart, R. F. & Pople, J. A. (1969). *J. Chem. Phys.* **51**, 2657–2664.

Hirshfeld, F. L. (1976). *Acta Cryst.* A**32**, 239–244.

Hirshfeld, F. L. & Hope, H. (1980). *Acta Cryst.* B**36**, 406–415.

Johnson, C. K. (1970). *Generalized Treatments for Thermal Motion*, ch. 9. Oxford University Press.

Johnson, C. K. (1976). *ORTEPII*. Report ORNL-5138. Tech. Rep., Oak Ridge National Laboratory, Tennessee, USA.

Luo, J., Ruble, J. R., Craven, B. M. & McMullan, R. K. (1996). *Acta Cryst.* B**52**, 357–368.

Madsen, A. Ø., Mason, S. & Larsen, S. (2003). *Acta Cryst.* B**59**, 653–663.

Madsen, D., Flensburg, C. & Larsen, S. (1998). *J. Phys. Chem. A*, **102**, 2177–2188.

Rousseau, B., Maes, S. T. & Lenstra, A. T. H. (2000). *Acta Cryst.* A**56**, 300–307.

Roversi, P., Barzaghi, M., Merati, F. & Destro, R. (1996). *Can. J. Chem.* **74**, 1145–1161.

Roversi, P. & Destro, M. (2004). *Chem. Phys. Lett.* **386**, 472–478.

Schomaker, V. & Trueblood, K. N. (1968). *Acta Cryst.* B**24**, 63–76.

Schomaker, V. & Trueblood, K. N. (1998). *Acta Cryst.* B**54**, 507–514.

Sheldrick, G. M. (1997). *SHELXL97. Program for the Refinement of Crystal Structures.* University of Göttingen, Germany.

Spackman, M. A. (1992). *Chem. Rev.* pp. 1769–1797.

Spackman, M. (1999*a*). *Chem. Phys. Lett.* **301**, 425–429.

Spackman, M. A. (1999*b*). *Acta Cryst.* A**55**, 30–47.

Spackman, M. A. & Byrom, P. G. (1996). *Acta Cryst.* B**52**, 1023–1035.

Stewart, R. F. (1976). *Acta Cryst.* A**32**, 182–185.

Stewart, R. F. (1991). *The Application of Charge Density Research to Chemistry and Drug Design*, edited by G. A. Jeffrey & J. F. Piniella, pp. 63–101. New York: Plenum Press.

Stewart, R. F., Davidson, E. R. & Simpson, W. T. (1965). *J. Chem. Phys.* **42**, 3175–3187.

Stewart, R. F., Spackman, M. A. & Flensburg, C. (1998). *VALRAY98 Users Manual.* Carnegie Mellon University, USA, and University of Copenhagen, Denmark.

Volkov, A., Abramov, Y. A. & Coppens, P. (2001). *Acta Cryst.* A**57**, 272–282.

Wal, R. J. van der & Stewart, R. F. (1984). *Acta Cryst.* A**40**, 587–593.

Weber, H.-P., Craven, B. M., Sawzip, P. & McMullan, R. K. (1991). *Acta Cryst.* B**47**, 116–127.

Wilson, A. J. C. & Prince, E. (1999). Editors. *International Tables for Crystallography*, Vol. C. Dordrecht: Kluwer Academic Publishers.